

1 A Fortran-Python Interface for Integrating Machine Learning Parameterization into  
2 Earth System Models

3 Tao Zhang<sup>1</sup>, Cyril Morcrette<sup>2,7</sup>, Meng Zhang<sup>3</sup>, Wuyin Lin<sup>1</sup>, Shaocheng Xie<sup>3</sup>, Ye Liu<sup>4</sup>, Kwinten Van  
4 Weverberg<sup>5,6</sup>, Joana Rodrigues<sup>2</sup>

- 5  
6 1. Brookhaven National Laboratory, Upton, NY, USA  
7 2. Met Office, FitzRoy Road, Exeter, EX13PB, UK  
8 3. Lawrence Livermore National Laboratory, Livermore, CA, USA  
9 4. Pacific Northwest National Laboratory, Richland, WA, USA  
10 5. Department of Geography, Ghent University, Belgium  
11 6. Royal Meteorological Institute of Belgium, Brussels, Belgium  
12 7. Department of Mathematics and Statistics, Exeter University, Exeter, UK  
13 Correspondence to: Tao Zhang (taozhang.ccs@gmail.com)

14 **Abstract**

15 Parameterizations in Earth System Models (ESMs) are subject to biases and uncertainties arising from  
16 subjective empirical assumptions and incomplete understanding of the underlying physical processes.  
17 Recently, the growing representational capability of machine learning (ML) in solving complex problems  
18 has spawned immense interests in climate science applications. Specifically, ML-based parameterizations  
19 have been developed to represent convection, radiation and microphysics processes in ESMs by learning  
20 from observations or high-resolution simulations, which have the potential to improve the accuracies and  
21 alleviate the uncertainties. Previous works have developed some surrogate models for these processes  
22 using ML. These surrogate models need to be coupled with the dynamical core of ESMs to investigate  
23 the effectiveness and their performance in a coupled system. In this study, we present a novel Fortran-  
24 Python interface designed to seamlessly integrate ML parameterizations into ESMs. This interface  
25 showcases high versatility by supporting popular ML frameworks like PyTorch, TensorFlow, and Scikit-  
26 learn. We demonstrate the interface's modularity and reusability through two cases: a ML trigger function  
27 for convection parameterization and a ML wildfire model. We conduct a comprehensive evaluation of  
28 memory usage and computational overhead resulting from the integration of Python codes into the  
29 Fortran ESMs. By leveraging this flexible interface, ML parameterizations can be effectively developed,  
30 tested, and integrated into ESMs.

31

## 32 Plain Language

33 Earth System Models (ESMs) are crucial for understanding and predicting climate change. However, they  
34 struggle to accurately simulate the climate due to uncertainties associated with parameterizing sub-grid  
35 physics. Although higher-resolution models can reduce some uncertainties, they require significant  
36 computational resources. Machine learning (ML) algorithms offer a solution by learning the important  
37 relationships and features from high-resolution models. These ML algorithms can then be used to develop  
38 parameterizations for coarser-resolution models, reducing computational and memory costs. To  
39 incorporate ML parameterizations into ESMs, we develop a Fortran-Python interface that allows for  
40 calling Python functions within Fortran-based ESMs. Through two case studies, this interface  
41 demonstrates its feasibility, modularity and effectiveness.

## 42 1. Introduction

43 Earth System Models (ESMs) play a crucial role in understanding the mechanism of the climate system  
44 and projecting future changes. However, uncertainties arising from parameterizations of sub-grid  
45 processes pose challenges to the reliability of model simulations (Hourdin et al., 2017). Kilometer-scale  
46 high-resolution models (Schär et al., 2020) can potentially mitigate the uncertainties by directly resolving  
47 some key subgrid-scale processes that need to be parameterized in conventional low-resolution ESMs.  
48 Another promising method, superparameterization – a type of multi-model framework (MMF) (D.  
49 Randall et al., 2003; D. A. Randall, 2013), explicitly resolves sub-grid processes by embedding high-  
50 resolution cloud-resolved models within the grid of low-resolution models. Consequently, both high-  
51 resolution models and superparameterization approaches have shown promise in improving the  
52 representation of cloud formation and precipitation. However, their implementation is challenged by  
53 exceedingly high computational costs.

54  
55 In recent years, machine learning (ML) techniques have emerged as a promising approach to  
56 improve parameterizations in ESMs. They are capable of learning complex patterns and  
57 relationships directly from observational data or high-resolution simulations, enabling the  
58 capture of nonlinearities and intricate interactions that may be challenging to represent with  
59 traditional parameterizations. For example, Zhang et al. (2021) proposed a ML trigger function  
60 for a deep convection parameterization by learning from field observations, demonstrating its  
61 superior accuracy compared to traditional CAPE-based trigger functions. Chen et al. (2023)  
62 developed a neural network-based cloud fraction parameterization, better predicting both spatial

63 distribution and vertical structure of cloud fraction when compared to the traditional Xu-Randall  
64 scheme (Xu & Randall, 1996). Krasnopolsky et al. (2013) prototyped a system using a neural  
65 network to learn the convective temperature and moisture tendencies from cloud-resolving  
66 model (CRM) simulations. These tendencies refer to the rates of change of various atmospheric  
67 variables over one time step, diagnosed from particular parameterization schemes. These studies  
68 lay the groundwork for integrating ML-based parameterization into ESMs.

69  
70 However, the aforementioned studies primarily focus on offline ML of parameterizations that do  
71 not directly interact with ESMs. Recently, there have been efforts to implement ML  
72 parameterizations that can be directly coupled with ESMs. Several studies have developed ML  
73 parameterizations in ESMs by hard coding custom neural network modules, such as O’Gorman  
74 & Dwyer (2018), Rasp et al. (2018), Han et al. (2020) and Gettelman et al. (2021). They  
75 incorporated a Fortran-based ML inference module to allow the loading of the pre-trained ML  
76 weights to reconstruct the ML algorithm in ESMs. The hard-coding has limitations. Such hard-  
77 coding approach restricts the ML algorithm’s ability to adapt to changes in the model dynamics  
78 over time, as the ‘online’ updating requires a two-way coupling between the dominantly Fortran-  
79 based ESMs and Python ML libraries.

80  
81 Fortran-Keras Bridge (FKB; Ott et al. (2020)) and C Foreign Function Interface (CFFI;  
82 <https://cffi.readthedocs.io>) are two packages that support two-way coupling between Fortran-based ESM  
83 and Python based ML parameterizations. FKB enables tight integration of Keras deep learning models but  
84 is specifically bound to the Keras library, limiting its compatibility with other frameworks like PyTorch  
85 and Scikit-Learn. On the other hand, CFFI provides a more flexible solution that in principle supports  
86 coupling various ML packages due to its language-agnostic design. Brenowitz & Bretherton (2018)  
87 utilized it to enable the calling of Python ML algorithms within ESMs. However, the CFFI has several  
88 limitations. When utilizing CFFI to interface Fortran and Python, it uses global data structures to pass  
89 variables between the two languages. This approach results in additional memory overhead as variable  
90 values need to be copied between languages, instead of being passed by reference. Additionally, CFFI  
91 lacks automatic garbage collection for the unused memory within these data structures and copies.  
92 Consequently, the memory usage of the program gradually increases over its lifetime. In addition, when  
93 using CFFI to call Python functions from a Fortran program, the process involves several steps such as  
94 registering variables into a global data structure, calling the Python function, and retrieving the calculated

**Deleted:** . Kochkov et al. (2023) presented an innovative ML parameterization that feeds back from the dynamics, in order to improve stability and reduce bias. However,

**Deleted:** s

99 result. These multiple steps can introduce computational overhead due to the additional operations  
100 required.

101  
102 Additionally, Wang et al. (2022) developed a coupler to facilitate two-way communication between ML  
103 parameterizations and host ESMs. The coupler gathers state variables from the ESM using the Message  
104 Passing Interface (MPI) and transfers them to a Python-based ML module. It then receives the output  
105 from the Python code and returns them to the ESM. While this approach effectively bridges Fortran and  
106 Python, its use of file-based data passing to exchange information between modules carries some  
107 performance overhead relative to tighter coupling techniques. Optimizing the data transfer, such as via  
108 shared memory, remains an area for improvement to fully leverage this coupler's ability to integrate  
109 online-adaptive ML parameterizations within large-scale ESM simulations, which is the main goal for this  
110 study.

111  
112 In this study, we investigate the integration of ML parameterizations into Fortran-based ESM  
113 models by establishing a flexible interface that enables the invocation of ML algorithms in  
114 Python from Fortran. This integration offers access to **any Python codes from Fortran, including**  
115 a diverse range of ML frameworks, **such as** PyTorch, TensorFlow, and Scikit-learn, which can  
116 effectively be utilized for parameterizing intricate atmospheric and other climate system  
117 processes. The coupling of the Fortran model and the Python ML code needs to be performed for  
118 thousands of model columns and over thousands of timesteps for a typical model simulation.  
119 Therefore, it is crucial for the coupling interface to be both robust and efficient. We showcase  
120 the feasibility and benefits of this approach through case studies that involve the  
121 parameterization of deep convection and wildfire processes in ESMs. The two cases demonstrate  
122 the robustness and efficiency of the coupling interface. The focus of this paper is on  
123 documenting the coupling between the Fortran ESM and the ML algorithms and systematically  
124 evaluating the computational efficiency and memory usage of different ML frameworks (such as  
125 Pytorch and TensorFlow), different ML algorithms, and different configuration of a climate  
126 model. The assessment of the scientific performance of the ML emulators will be addressed in  
127 follow-on papers. The showcase examples emphasize the potential for high modularity and  
128 reusability by separating the ML components into Python modules. This modular design  
129 facilitates independent development and testing of ML-based parameterizations by researchers. It  
130 enables easier code maintenance, updates, and the adoption of state-of-the-art ML techniques

Deleted: including

132 with ~~only minimal~~ disrupting the existing Fortran infrastructure. Ultimately, this advancement  
133 will contribute to enhanced predictions and a deeper comprehension of the evolving climate of  
134 our planet. ~~It is important to note that the current interface only supports executing deep learning~~  
135 ~~algorithms on CPUs and does not support running them on GPUs.~~

Deleted: out

Deleted: important to note

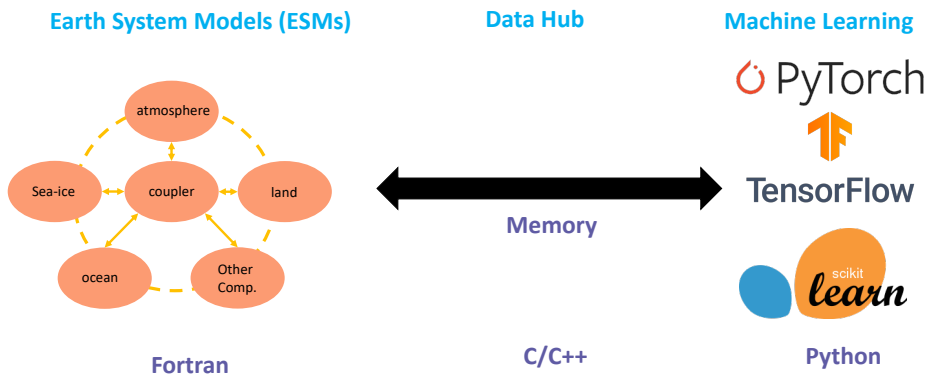
Deleted: ¶

136  
137 The rest of this manuscript is organized as follows: Section 2 presents the detailed interface that  
138 integrates ML into Fortran-based ESM models. Section 3 discusses the performance of the  
139 interface and presents its application in two case studies. Finally, Section 4 provides a summary  
140 of the findings and a discussion of their implications.

## 141 2. General design of the ML interface

### 142 2.1 Architecture of the ML interface

143 We developed an interface using shared memory to enable two-way coupling between Fortran and Python  
144 (Figure 1). The ESM used in the demonstration in Figure 1 is the U.S. Department of Energy (DOE)  
145 Energy Exascale Earth System Model (E3SM; Golaz et al., 2019, 2022). Because Fortran cannot directly  
146 call Python, we utilized C as an intermediary since Fortran can call C functions. This approach leverages  
147 C as a data hub to exchange information without requiring a framework-specific binding like KFB. As a  
148 result, our interface supports invoking any Python-based ML package such as PyTorch, TensorFlow, and  
149 scikit-learn from Fortran. While C can access Python scalar values through the built-in  
150 PyObject\_CallObject function from the Python C API, we employed Cython for its ability to transfer  
151 array data between the languages. Using Cython, multidimensional data structures can be efficiently  
152 passed between Fortran and Python modules via C, allowing for flexible training of ML algorithms within  
153 ESMs.



157  
 158 **Figure 1.** The interface of the ML bridge for two-way communication via memory between Fortran ESM  
 159 and Python ML module.

160 **2.2 Code structure**

161 Figure 2 illustrates how the framework operates using toy code example. The Fortran-Python interface  
 162 comprises a Fortran wrapper and C wrapper files, which are bound together. The Fortran-based ESM first  
 163 imports the Fortran wrapper, allowing it to call wrapper functions with input and output memory  
 164 addresses. The interface then passes these memory addresses to the Python-based ML module, which  
 165 performs the ML predictions and returns the output address to the Fortran model.

```

    Fortran-Python Interface
    module ml_wrapper
    interface
    function ml_wrap_f(pcols,pver,t,varo)
    bind(C_name="wrap_ml_c")
    use iso_c_binding
    declare these variables
    end function ml_wrap_f
    end module ml_wrapper
    ml_wrap.f90

    #include <stdio.h>
    #include <Python.h>
    #include "ml_py.h"
    double ml_wrap_c(int pcols, int pver,
    double **t, double **varo)
    {
    python initialize
    varo = calc_cape(pcols,pver,t);
    return 1.0;
    }
    ml_wrap.c.c

    ESM model (Fortran)
    program example
    ! import the ml_wrapper, use the ml_wrapper module
    use ml_wrapper

    !call the fortran wrapper function
    j = wrap_ml_f(pcols,pver,t,varo)
    end program simple
    main.f90

    ML (Python)
    cdef public double calc_cape(int
    pcols,int pver,double **t, double
    **varo):
    varo = do_ML(pver, pcols, t)
    return &varo
    ml_py.pyx
  
```

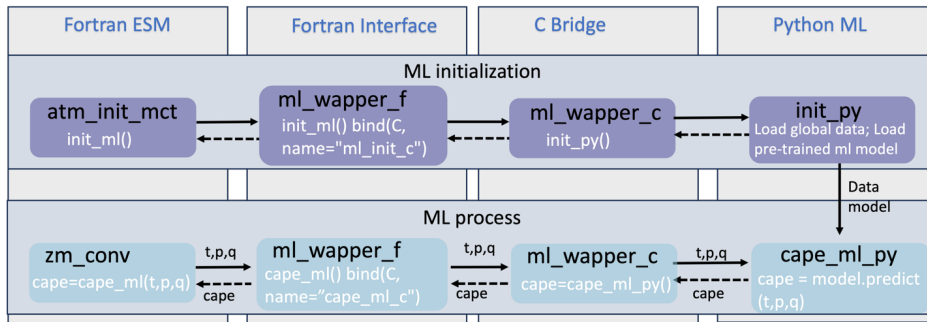
Annotations in the code block:

- 1. Call the python func. (points to `python initialize` in `ml_wrap.c.c`)
- 2. Call the fortran wrapper func. (points to `use ml_wrapper` in `main.f90`)
- 3. Bind with a func. (points to `bind(C_name="wrap_ml_c")` in `ml_wrapper`)
- 4. Call the python func. (points to `return &varo` in `ml_py.pyx`)

166  
 167 **Figure 2.** Toy code illustrating the Fortran-Python interface.

Formatted: Font: (Default) Arial, (Asian) Arial  
 Formatted: Centered

168  
 169 When coupling the Python ML module with the real model using the interface, additional steps should be  
 170 considered: 1. The ML module should remain active throughout the model simulations, without any  
 171 Python finalization calls, ensuring it is continuously available. 2. The Python module should load the  
 172 trained ML model and any required global data only once, rather than at each simulation step. This one-  
 173 time initialization process improves efficiency and prevents unnecessary repetition. On the Fortran ESM  
 174 side, the `init_ml()` function is called within the `atm_init_mct` module to load the ML model and global  
 175 data (shown in Figure 3). Then, similar to the toy code, we call the wrapper function, pass input variables  
 176 to Python for ML predictions, and return the results to the Fortran side. 3. When compiling the complex  
 177 system, which includes Python, C, Cython, and Fortran code, the Python path should be specified in the  
 178 CFLAGS and LDFLAGS. It is important to note that without the position-independent compiling flag (`-fPIC`), the hybrid system will only work on a single node and may cause segmentation faults on multiple  
 179 nodes. Including it can resolve this issue, allowing multi-node compatibility.  
 180



183  
 184 **Figure 3.** The code structure of the ML bridge interface using the ML closure in deep convection as an  
 185 example.  
 186

187 In traditional ESMs, sub-grid scale parameterization routines such as convection parameterizations are  
 188 often calculated separately for each vertical column of the model domain. Meanwhile, the domain is  
 189 typically decomposed horizontally into 2D chunks that can be solved in parallel using MPI processes.  
 190 Each CPU core/MPI process is assigned a number of chunks of model columns to update asynchronously  
 191 (Figure 4). Our interface takes advantage of this existing parallel decomposition by designing the ML  
 192 calls to operate over all columns simultaneously within each chunk, rather than invoking the ML scheme  
 193 individually for each column. This allows the coupled model-ML system to leverage parallelism in the

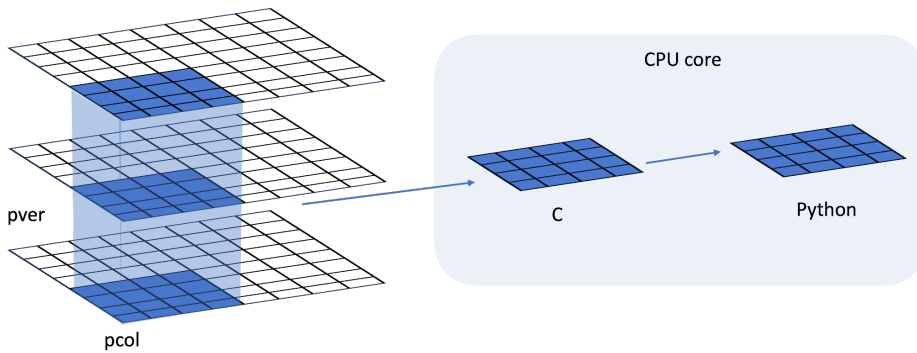
**Deleted:** The interface consists of two stages. The first stage involves initializing the ML environment, which persists throughout the model simulations. On the Fortran ESM side, the `init_ml()` function is called in the `atm_init_mct` module. Through the Fortran Interface and C Bridge, the corresponding function in the Python ML component is invoked. This function loads the ML-related global data and the trained ML algorithm. This initialization process is performed only once to enhance efficiency and avoid unnecessary repetition during the simulations. The second stage involves the actual invocation of the ML process. The example here is an ML-based closure for the deep convection parameterization. We aim to utilize ML to calculate Convective Available Potential Energy (CAPE) by utilizing an ML emulator based on high-resolution cloud-resolving model simulations. We call the `cape_ml` function in the Fortran module `zm_conv`, providing temperature, pressure, and humidity as input variables, and defining the returned CAPE from the ML side. Through the Fortran Interface and C Bridge, these three variables are passed to the Python ML component. In the Python ML component, the received variables, along with other pre-loaded global data and the trained ML algorithm, are used to calculate the ML-based CAPE. The calculated result is then returned to the Fortran ESM. The Fortran ESM utilizes this ML-derived CAPE to determine how convection will evolve.

**Deleted:** 1

**Deleted:** 2

**Deleted:** 3

223 neural network computations. If the ML were called separately for every column, parallel efficiencies  
 224 would not be realized. By aggregating inputs over the chunk-scale prior to interfacing with Python,  
 225 performance is improved through better utilization of multi-core and GPU-based ML capabilities during  
 226 parameterization calculations.



228 **Figure 4.** Data and system structure. The model domain is decomposed into chunks of columns. pver  
 229 refers to number of pressure vertical levels. A chunk contains multiple columns (up to pcol). Multiple  
 230 chunks can be assigned to each CPU core.

### 234 3. Results

235 The framework explained in the previous section provides seamless support for various ML  
 236 parameterizations and various ML frameworks, such as PyTorch, Tensorflow, and Scikit-learn. To  
 237 demonstrate the versatility of this framework, we applied it in two distinct case applications. The first  
 238 application replaces the conventional CAPE-based trigger function in a deep convection parameterization  
 239 with a machine-learned trigger function. The second application involves a ML-based wildfire model that  
 240 interacts bidirectionally with the ESM. We provide a brief introduction to these two cases. Detailed  
 241 descriptions and evaluations will be presented in separate papers.

242  
 243 The framework's performance is influenced by two primary factors: increasing memory usage and  
 244 increasing computational overhead. Firstly, maintaining the Python environment fully persistent in  
 245 memory throughout model simulations can impact memory usage, especially for large ML algorithms.

**Deleted:** The Python, C, Cython and Fortran code components are compiled together into a unified executable file. Table 1 shows the detailed steps to enable the ML bridge interface in E3SM.

**Deleted:** 3

**Deleted:** Table 1. The steps to enable the ML bridge framework in E3SM

**Deleted:** ¶

**Formatted:** Font: (Default) Arial, (Asian) Arial

**Formatted:** Centered

**Deleted:** t



255 This elevated memory footprint increases the risk of leaks or crashes as simulations progress. Secondly,  
256 executing ML components within the Python interpreter inevitably introduces some overhead compared  
257 to the original ESMs. The increased memory requirements and decreased computational efficiency  
258 associated with these considerations can impact the framework's usability, flexibility, and scalability for  
259 different applications.

260  
261 To comprehensively assess performance, we conducted a systematic evaluation of various ML  
262 frameworks, ML algorithms, and physical models. This evaluation is built upon the foundations  
263 established for evaluating the ML trigger function in the deep convection parameterization.

## 264 3.1 Application cases

### 265 3.1.1 ML trigger function in deep convection parameterization

266 In General Circulation Models, uncertainties in convection parameterizations are recognized to be closely  
267 linked to the convection trigger function used in these schemes (Bechtold et al., 2004; Xie et al., 2004,  
268 2019; Xie & Zhang, 2000; Lee et al., 2007). The convective trigger in a convective parameterization  
269 determines when and where model convection should be triggered as the simulation advances. In many  
270 convection parameterizations, the trigger function consists of a simple, arbitrary threshold for a physical  
271 quantity, such as convective available potential energy (CAPE). Convection will be triggered if the  
272 CAPE value exceeds a threshold value.

273  
274 In this work, we use this interface to test a newly developed ML trigger function in E3SM. The ML  
275 trigger function was developed with the training data originating from simulations performed using the  
276 kilometer-resolution (1.5 km grid spacing). Met Office Unified Model Regional Atmosphere 1.0  
277 configuration (Bush et al., 2020). Each simulation consists of a limited area model (LAM) nested within a  
278 global forecast model providing boundary conditions (Walters et al., 2017; Webster et al., 2008). In total  
279 80 LAM simulations were run located so as to sample different geographical regions worldwide. Each  
280 LAM was run for 1 month, with 2-hourly output, using a grid-length of 1.5 km, a 512 x 512 domain, and  
281 a model physics package used for operational weather forecasting. The 1.5 km data is coarse-grained to  
282 several scales from 15 to 144 km.

283  
284 A two-stream neural network architecture is used for the ML model. The first stream takes profiles of  
285 temperature, specific humidity and pressure across 72 levels at each scale as inputs and passes them  
286 through a 4-layer convolutional neural network (CNN) with kernel sizes of 3, to extract large scale

**Deleted:** Convection plays a vital role in atmospheric processes, such as precipitation formation, heat and moisture transport, and energy redistribution (Arakawa, 2004; Arakawa & Schubert, 1974). However, the deficiencies in convection parameterizations constitute one of the principal sources of uncertainties

**Deleted:** i

**Deleted:** (D. A. Randall, 2013). Some

**Deleted:** Figure 4a illustrates how the CAPE-based trigger function works

**Deleted:**, such as 70 J/kg used in E3SM version 1

**Deleted:** and apply it to

**Deleted:**

**Deleted:** The ML trigger function was developed with

**Deleted:**

**Deleted:** t

**Deleted:**

**Deleted:** originating

**Deleted:**

**Deleted:** This physics package does not include a convective parameterization scheme, but does include a representation of fractional cloudiness (Bush et al., 2020).

**Deleted:**, comparable to the scale a global model might be run at

**Deleted:** At each scale,

**Deleted:** we assess whether individual pixels can be considered to be buoyant cloudy updrafts (BCU, e.g. Hartmann et al., 2019; Swann, 2001). Here, the threshold for buoyant is local virtual temperature more than 0.1 K warmer than the average at that scale and height. Cloudy is defined whenever the fractional cloud cover is greater than 0.0 and updraft is defined as vertical ascent larger than 0.2 m/s. In each averaging region, the number of grid points that meet all three criteria are counted and saved as a profile of BCU fraction.

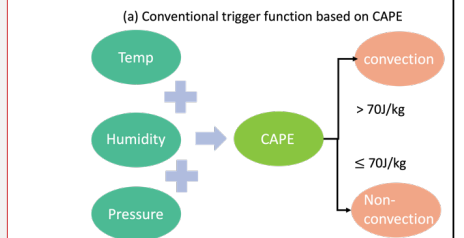
**Deleted:** †

323 features. The second stream takes mean orographic height, standard deviation of orographic height, land  
 324 fraction and the size of the grid-box as inputs. The outputs of the two streams are then combined and fed  
 325 into a 2-layer fully connected network to allow the ML model to leverage both atmospheric and surface  
 326 features when making its predictions. The output is a binary variable indicating whether the convection  
 327 happens, based on the condition of buoyant cloudy updrafts (BCU, e.g. Hartmann et al., 2019; Swann,  
 328 2001). If there are 3 contiguous levels where the predicted BCU is larger than 0.05, the convection  
 329 scheme is triggered. Once trained, the CNN is coupled to E3SM and thermodynamic information from  
 330 E3SM is passed to it to predict the trigger condition. Then, the predicted result is returned to E3SM.

**Deleted:** The output of the ML model is a profile of BCU.

**Deleted:** the profile of BCU. If there are 3 contiguous levels where the predicted BCU is larger than 0.05, the convection scheme is triggered.

332  
 333  
 334 Figure 5 shows the comparison of annual mean precipitation between the control run using the traditional  
 335 CAPE-based trigger function and the run using the ML BCU trigger function. The ML BCU scheme  
 336 demonstrates reasonable spatial patterns of precipitation, similar to the control run, with comparable root-  
 337 mean-square error and spatial correlation. Additional experiments exploring the definition of BCU and  
 338 varying the thresholds along with an in-depth analysis will be presented in a follow-up paper.



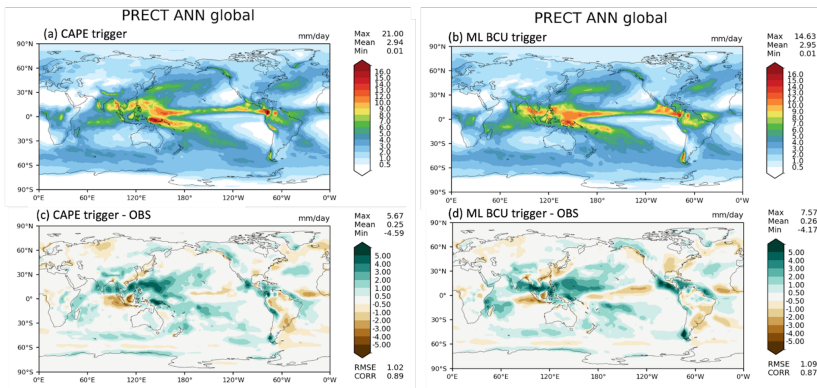
**Deleted:**

**Deleted:** Figure 4. Structure of traditional CAPE-based and the new ML BCU-based trigger function. The rectangles in LAM represent the LAM domains.

**Deleted:**

**Deleted:** The ML trigger function is implemented using this two-stream architecture and coupled with the E3SM model using the framework described in Section 2.

**Deleted:**



340  
 341 **Figure 5.** Comparison of annual mean precipitation between the control run using the CAPE-based  
 342 trigger function (a, c) and the run using the ML BCU trigger function (b, d).

### 343 3.1.2 ML learning fire model

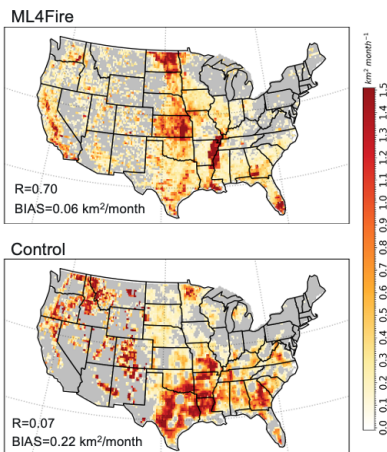
344 Predicting wildfire burned area is challenging due to the complex interrelationships between fires,  
 345 climate, weather, vegetation, topography, and human activities (Huang et al., 2020). Traditionally,

**Deleted:** Wildfires in the United States have significantly increased in frequency and intensity in recent decades, resulting in substantial direct and indirect losses (Iglesias et al., 2022). ...

363 statistical methods like multiple linear regression have been applied, but are limited in the number and  
 364 diversity of predictors considered (Yue et al., 2013). In this study, we develop a coupled fire-land-  
 365 atmosphere framework that uses machine learning to predict wildfire area, enhancing long-term burned  
 366 area projections and assessing fire impacts by enabling simulations of interactions among fire,  
 367 atmosphere, land cover, and vegetation.

369 The ML algorithm is trained using a monthly dataset, which includes the target variable of burned area, as  
 370 well as various predictor variables. These predictors encompass local meteorological data (e.g., surface  
 371 temperature, precipitation), land surface properties (e.g., monthly mean evapotranspiration and surface  
 372 soil moisture), and socioeconomic variables (e.g., gross domestic product, population density), as  
 373 described by Wang et al. (2022). In the coupled fire-land-atmosphere framework, meteorology variables  
 374 and land surface properties are provided by the E3SM. We use the eXtreme Gradient Boosting algorithm  
 375 implemented in Scikit-Learn to train the ML fire model. Figure 6 demonstrates that the ML4Fire model  
 376 exhibits superior performance in terms of spatial distribution compared to process-based fire models,  
 377 particularly in the Southern US region. Detailed analysis will be presented in a separate paper. The  
 378 ML4Fire model has proven to be a valuable tool for studying vegetation-fire interactions, enabling  
 379 seamless exploration of climate-fire feedbacks.

380  
 381

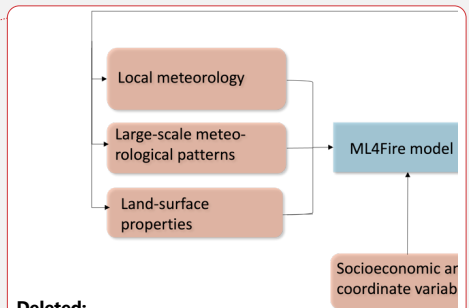


382

**Deleted:** Alternatively, ML algorithms that capture statistical relationships between the burned area and environmental factors have shown promising burned area prediction (Kondylatos et al., 2022; Li et al., 2023; Wang et al., 2022, 2023). However, improving long-term burned area projections and evaluating fire impacts requires the coupling of the fire model to an earth system model, which allows simulations of the interactions between the fire, atmosphere, land cover and vegetation (Huang et al., 2021). To achieve this, we develop a coupled fire-land-atmosphere framework using ML. ...

**Deleted:** , as illustrated in Figure 6

**Deleted:** 7



**Deleted:**

**Deleted:** Figure 6. Structure of ML fire model (ML4Fire) coupled into E3SM model.

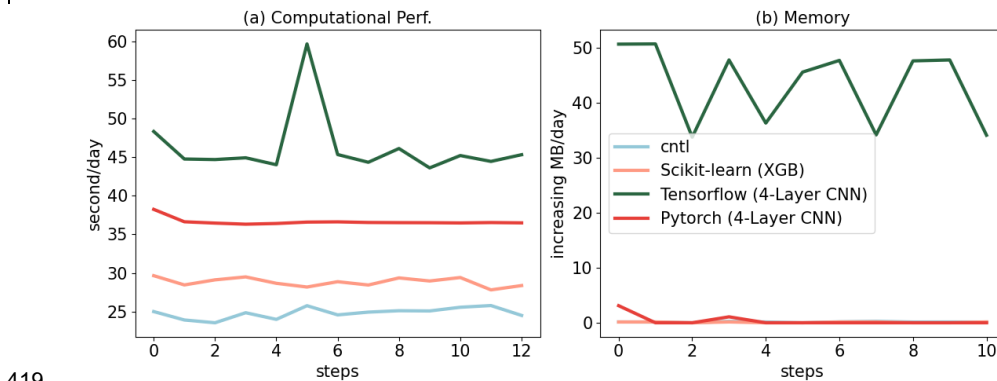
**Deleted:** †

400 **Figure 6.** Comparison between ML4Fire model and process-based fire model against the historical  
401 burned area from Global Fire Emissions Database 5 from 2001-2020. R and BIAS are the spatial  
402 pattern correlation and difference against the observation, respectively.

Deleted: 7

### 403 3.2 Performance of different ML frameworks

404 The Fortran-Python bridge ML interface supports various ML frameworks, including PyTorch,  
405 TensorFlow, and scikit-learn. These ML frameworks can be trained offline using kilometer-scale high-  
406 resolution models (such as the ML trigger function) or observations (ML fire model). Once trained, they  
407 can be plugged into the ML bridge interface through different API interfaces specific to each framework.  
408 The coupled ML algorithms are persistently resident in memory, just like the other ESM components.  
409 During each step of the process, the performance of the full system is significantly affected by memory  
410 usage. If memory consumption increases substantially, it may lead to memory leaks as the number of time  
411 step iteration increases. In addition, Python, being an interpreted language, is typically considered to have  
412 slower performance compared to compiled languages like C/C++ and Fortran. Therefore, incorporating  
413 Python may decrease computational performance. We examine the memory usage and computational  
414 performance across various ML frameworks based on implementing the ML trigger function in E3SM.  
415 The ML algorithm is implemented as a two-stream CNN model using Pytorch and TensorFlow  
416 frameworks, as well as XGBoost using the Scikit-learn package. It should be noted that XGBoost, a  
417 boosting tree-based model, is a completely different type of ML model compared to the CNNs, which are  
418 the type of deep neural network.



419 **Figure 7.** Computational and memory overhead as the simulation progresses for coupling the ML trigger  
420 function with the E3SM model. The x-axis represents the simulated time step. The y-axis of (a) represents  
421 the simulation speed measured in seconds per day (indicating the number of seconds required to simulate  
422 one day). The y-axis of (b) represents the relative increase in memory usage for Scikit-learn, TensorFlow,  
423

Deleted: 8

426 and PyTorch compared with CNTL. CNTL represents the original simulation without using the ML  
427 framework.

429 Figure 7 illustrates the computational and memory overhead associated with the ML parameterization  
430 using different ML frameworks. It shows that XGBoost only exhibits a 20% increase in the simulation  
431 time required for simulating one day due to its simpler algorithm. For more complex neural networks,  
432 PyTorch incurs a 52% overhead, while TensorFlow's overhead is almost 100% – about two times as much  
433 as the overhead by PyTorch. In terms of memory usage, we use the highwater memory metric (Gerber &  
434 Wasserman, 2013), which represents the total memory footprint of a process. Scikit-learn and PyTorch do  
435 not show any significant increase in memory usage. However, TensorFlow shows a considerable increase  
436 up to 50MB per simulation day per MPI process element. This is significant because for a node with 48  
437 cores, it would equate to an increase of around 2GB per simulated day on that node. This rapid memory  
438 growth could quickly lead to a simulation crash due to insufficient memory during continuous  
439 integrations, preventing the use in practical simulations. Our findings show that the TensorFlow  
440 prediction function does not release memory after each call. Therefore, we recommend using PyTorch for  
441 complex deep learning algorithms and Scikit-learn for simpler ML algorithms to avoid these potential  
442 memory-related issues when using TensorFlow.

443  
444 Previous work, such as Brenowitz & Bretherton (2018, 2019) has utilized the CFFI package to establish  
445 communication between Fortran ESM and ML Python. As described in the Introduction, while CFFI  
446 offers flexibility in supporting various ML packages, it does have certain limitations. To pass variables  
447 from Fortran to Python, the approach relies on global data structures to store all variables, including both  
448 the input from Fortran to Python and the output returning to Fortran. Consequently, this package results in  
449 additional memory copy operations and increasing overall memory usage. In contrast, our interface takes  
450 a different approach by utilizing memory references to transfer data between Fortran and Python,  
451 avoiding the need for global data structures and the associated overhead. This allows for a more efficient  
452 data transfer process.

453  
454 In Figure 8, we present a comparison between the two frameworks by testing the different number of  
455 elements passed from Fortran to Python. The evaluation is based on a demo example that focuses solely  
456 on declaring arrays and transferring them from Fortran to Python, rather than a real E3SM simulation.

457 Figure 8a illustrates the impact of the number of passing elements on the overhead of the two interfaces.  
458 As the number of elements exceeds  $10^4$ , the overhead of CFFI becomes significant. When the number  
459 surpasses  $10^6$ , the overhead of CFFI is nearly ten times greater than that of our interface. Regarding

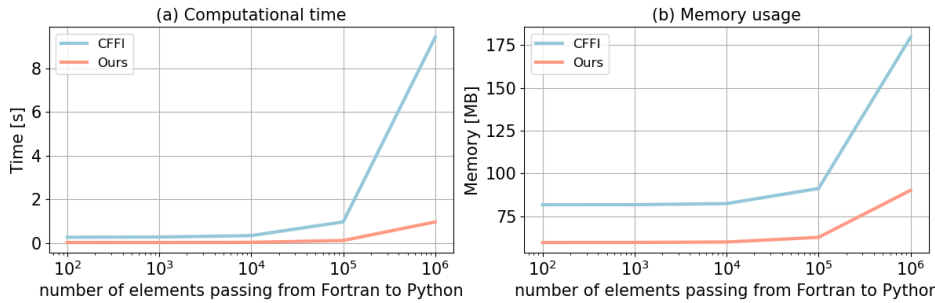
Deleted: 8

Deleted:

Deleted:

Deleted:

464 memory usage, our interface maintains a stable memory footprint of approximately 60MB. Even as the  
 465 number of elements increases, the memory usage only shows minimal growth. However, for CFFI, the  
 466 memory usage starts at 80MB, which is 33% higher than our interface. As the number of elements  
 467 reaches  $10^6$ , the memory overhead for CFFI dramatically rises to 180MB, twice as much as our interface.  
 468



469  
 470 Figure 8. Comparison of our framework and the CFFI framework in terms of computational time  
 471 and memory usage. The x-axis represents the number of elements transferred from Fortran to  
 472 Python, while the y-axis displays the total time (a) and total memory usage (b) for a  
 473 demonstration example. The evaluations presented are based on the average results obtained  
 474 from 5 separate tests.  
 475

Deleted:

Deleted: 9

### 476 3.3 Performance of ML algorithms of different complexities

477 ML parameterizations can be implemented using various deep learning algorithms with different levels of  
 478 complexity. The computational performance and memory usage can be influenced by the complexity of  
 479 these algorithms. In the case of the ML trigger function, a two-stream four-layer CNN structure is  
 480 employed. We compare this structure with other ML algorithms such as Artificial Neural Network (ANN)  
 481 and Residual Network (ResNet), whose structures are detailed in Table 1. We selected these three ML  
 482 algorithms because they are commonly used in previous ML parameterization approaches, such as  
 483 (Brenowitz & Bretherton, 2019; Han et al., 2020; Wang et al., 2022). Systematically evaluating the hybrid  
 484 system with these ML methods using our interface can help identify bottlenecks and improve the system  
 485 computational performance. These algorithms are implemented in PyTorch. The algorithm's complexity  
 486 is measured by the number of parameters, with the CNN having approximately 60 times more parameters  
 487 than ANN, and ResNet having roughly 1.5 times more parameters than CNN.  
 488

Deleted: 2

492 **Table 1.** The structure and number of parameters of each ML algorithms.

Algorithms	Structure	# of parameters
ANN	3 x Linear	121,601
CNN	4 x Conv2d + 2 x Linear	7,466,753
ResNet	17 x Conv2d + 1 x Linear	11,177,025

Deleted: 2

493  
494 Figure 9<sub>a</sub> presents a comparison of the memory and computational costs between the CNTL run without  
495 deep learning parameterization and the hybrid run with various deep learning algorithms. The same  
496 specific process-element layout (placement of ESM component models on distributed CPU cores) is used  
497 for all the simulations. Deep learning algorithms incur a significant yet affordable increase in memory  
498 overhead, with at least a 20% increase compared to the CNTL run (Figure 9<sub>a</sub>). This is primarily due to the  
499 integration of ML algorithms into the ESM, which persist throughout the simulations. Although there is a  
500 notable increase in complexity among the deep learning algorithms, their memory usage only shows a  
501 slight rise. This is because the memory increment resulting from the ML parameters is relatively small.  
502 Specifically, ANN requires 1MB of memory, CNN requires 60MB, and the ResNet algorithms requires  
503 85MB, which are calculated based on the number of parameters in each algorithm. When comparing these  
504 values to the memory consumption of the CNTL run, which is approximately 3000MB, the additional  
505 parameters' incremental memory consumption is not substantial. However, when we use 128 MPI  
506 processes per node, it could bring the total memory requirement to approximately 460 GB per node. If the  
507 available hardware memory is less than this, the process layout must be adjusted accordingly.

Deleted: 10

Deleted: A

Deleted: 10

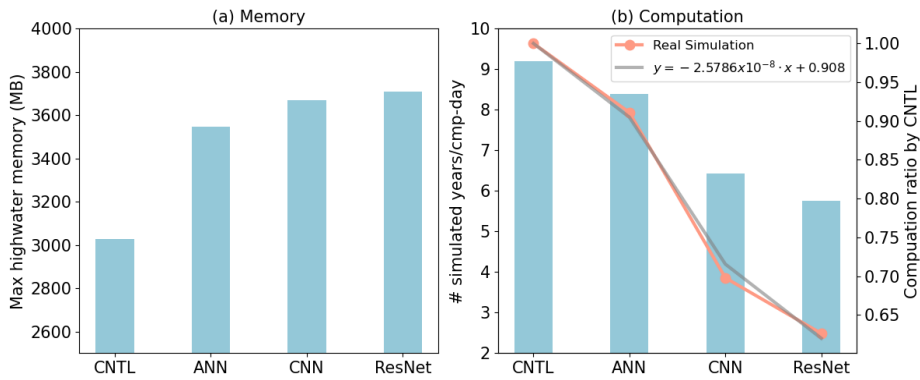
509 In terms of computational performance, the Python-based ML calls inevitably introduce some overhead.  
510 However, as shown in Figure 9b, the performance decrease is not substantial. The simple ANN model  
511 reduces performance by only about 10% compared to the CNTL run, while even the more complex  
512 ResNet model results in a 35% decrease. In contrast, Wang et al. (2022) reported a 100% overhead in  
513 their interface, which transfers parameters via files. It is worth noting that in this study, the deep learning  
514 algorithms are executed on CPUs. To enhance computational performance, future work could consider  
515 utilizing GPUs for acceleration.

Deleted: However, there is a significant decrease in computational performance as the complexity of the deep learning algorithms increases (Figure 10b). This is primarily due to the larger number of parameters in neural networks, which require more forward computations

Deleted: .

516  
517 In addition, we develop a performance model to estimate computational performance for the hybrid  
518 model using different ML model sizes and complexities. This performance model, based on linear  
519 regression, predicts the computational ratio relative to the CNTL run by taking the number of ML

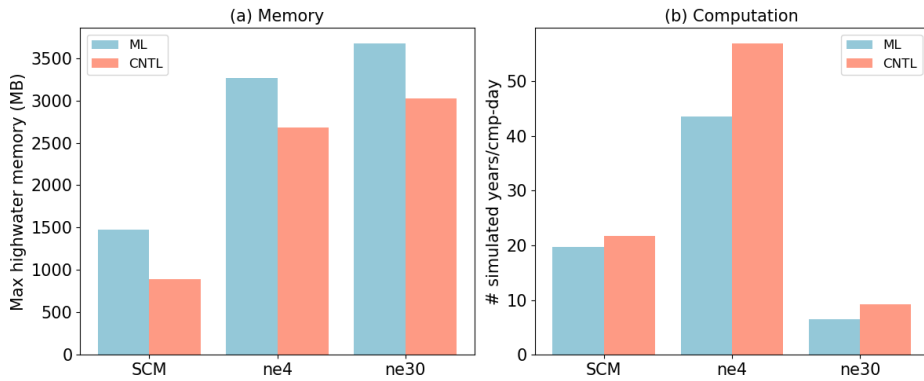
530 parameters as input, shown in Figure 9b. It provides a simple yet effective way to capture this relationship  
 531 and serves as a valuable tool for performance prediction when incorporating more complicated ML  
 532 models.



533  
 534 **Figure 9.** Comparison of CNTL and the hybrid model using various ML algorithms in terms of memory  
 535 and computation. CNTL is the default run without ML parameterizations. In (b), the left y-axis represents  
 536 the actual number of simulated years per day, while the right y-axis shows the relative performance  
 537 compared to the CNTL run (orange line). The gray line illustrates the regression between the number of  
 538 ML parameters (x) and the relative performance of the hybrid system (y).

Deleted: 10

540 3.4 Performance for physical models of different complexities



541



543 **Figure 10.** Comparison of CNTL and ML for various ESMs in terms of memory and computation. The  
544 ESM configuration include SCM, ultra-low resolution model (ne4) and nominal low-resolution model  
545 (ne30).

Deleted: 11

546  
547 ML parameterization can be applied to various ESM configurations, for example, with the E3SM  
548 Atmosphere Model (EAM), we experiment with Single Column Model (SCM), the ultra low-resolution  
549 model of EAM (ne4), and the nominal low resolution model of EAM (ne30) configurations. The SCM  
550 consists of one single atmosphere column of a global EAM (Bogenschutz et al., 2020; Gettelman et al.,  
551 2019). ne4 has 384 columns, with each column representing the horizontal resolution of 7.5°. ne30 is the  
552 default resolution for EAM and comprises 21,600 columns, with each column representing the horizontal  
553 resolution of 1°. In the case of the ML trigger function, the memory overhead is approximately 500MB  
554 for all configurations due to the loading of the ML algorithm, which does not vary with the configuration  
555 of the ESM.

556  
557 Regarding computational performance, SCM utilizes 1 process, ne4 employs 1 node with 64 processes,  
558 and ne30 utilizes 10 nodes with each node using 128 processes. In the case of SCM, the overhead  
559 attributed to the ML parameterization is approximately 9% due to the utilization of only 1 process.

560 However, for ne4 and ne30, the overhead is 23% and 28% respectively (Figure 10). The increasing  
561 computational overhead is primarily due to resource competition when multiple processes are used within  
562 a single node. It is noted that although there is a significant computational gap between ML and CNTL  
563 for ne4, the relative performance between ML and CNTL for ne4 is approximately 76.7%, which is close  
564 to ne30 at 71.4%.

Deleted: 11

## 566 4. Discussion and Conclusion

567 ML algorithm can learn detailed information about cloud processes and atmospheric dynamics from  
568 kilometer-scale models and observations and serves as an approximate surrogate for the kilometer-scale  
569 model. Instead of explicitly simulating kilometer-scale processes, the ML algorithms can be designed to  
570 capture the essential features and relationships between atmospheric variables by training on available  
571 kilometer-scale data. The trained algorithms can then be used to develop parameterizations for use in  
572 models at coarser resolutions, reducing the computational and memory costs. By using ML  
573 parameterizations, scientists can effectively incorporate the insights gained from kilometer-scale models  
574 for coarser-resolution simulations. Through learning the complex relationships and patterns present in the

Deleted: In this study, we develop a novel Fortran-Python interface for developing ML parameterizations.

579 high-resolution data, the ML-based parameterizations have the potentials to more accurately represent  
580 cloud processes and atmospheric dynamics in the ESMs. This approach strikes a balance between  
581 computational efficiency and capturing critical processes, enabling more realistic simulations and  
582 predictions while minimizing computational resources. All these potential benefits in turn promote  
583 innovative developments to facilitate increasing and more efficient use of ML parameterizations.

584  
585 In this study, we develop a novel Fortran-Python interface for developing ML parameterizations. This  
586 interface demonstrates feasibility in supporting various ML frameworks, such as PyTorch, TensorFlow,  
587 and Scikit-learn and enables the effective development of new ML-based parameterizations to explore  
588 ML-based applications in ESMs. Through two cases - a ML trigger function in convection  
589 parameterization and a ML wildfire model - we highlight high modularity and reusability of the  
590 framework. We conduct a systematic evaluation of memory usage and computational overhead from the  
591 integrated Python codes.

592  
593 Based on our performance evaluation, we observe that coupling ML algorithms using TensorFlow into  
594 ESMs can lead to memory leaks. As a recommendation, we suggest using PyTorch for complex deep  
595 learning algorithms and Scikit-learn for simple ML algorithms for the Fortran-Python ML interface.

596  
597 The memory overhead primarily arises from loading ML algorithms into ESMs. If the ML algorithms are  
598 implemented using PyTorch or Scikit-learn, the memory usage will not increase significantly. The  
599 computational overhead is influenced by the complexity of the neural network and the number of  
600 processes running on a single node. As the complexity of the neural network increases, more parameters  
601 in the neural network require forward computation. Similarly, when there are more processes running on  
602 a single node, the integrated Python codes introduce more resource competition.

603  
604 Although this interface provides a flexible tool for ML parameterizations, it does not currently utilize  
605 GPUs for ML algorithms. In Figure 3, it is shown that each chunk is assigned to a CPU core. However, to  
606 effectively leverage GPUs, it is necessary to gather the variables from multiple chunks and pass them to  
607 the GPUs. Additionally, if an ESM calls the Python ML module multiple times in each time step, the  
608 computational overhead becomes significant. It is crucial to gather the variables and minimize the number  
609 of calls. In the future, we will enhance the framework to support this mechanism, enabling GPU  
610 utilization and overall performance improvement.

Deleted: gradient

## 612 Acknowledge

613 This work was primarily supported by the Energy Exascale Earth System Model (E3SM) project of the  
614 Earth and Environmental System Modeling program, funded by the US Department of Energy, Office of  
615 Science, Office of Biological and Environmental Research. Research activity at BNL was under the  
616 Brookhaven National Laboratory contract DE-SC0012704 (Tao Zhang, Wuyin Lin). The work at LLNL  
617 was performed under the auspices of the US Department of Energy by the Lawrence Livermore National  
618 Laboratory under Contract DE-AC52-07NA27344. The work at PNNL is performed under the Laboratory  
619 Directed Research and Development Program at the Pacific Northwest National Laboratory. PNNL is  
620 operated by DOE by the Battelle Memorial Institute under contract DE-A05-76RL01830.

621

## 622 Author contribution

623 TZ developed the Fortran-Python Interface. CM and JR contributed the ML model for the trigger  
624 function. YL contributed the ML model for the wire fire model. TZ and MZ assessed the performance of  
625 the ML trigger function. TZ took the lead in preparing the manuscript, with valuable edits from CM, MZ,  
626 WL, SX, YL, KW, and JR. All the co-authors provided valuable insights and comments for the  
627 manuscript.

## 628 Conflict of Interest

629 The authors declare that they have no conflict of interest.

630

## 631 Data Availability Statement

632 The Fortran-Python interface for developing ML parameterizations can be archived at  
633 <https://doi.org/10.5281/zenodo.11005103> (Zhang et al., 2024) and can be also accessed at  
634 <https://github.com/tzhang-ccs/ML4ESM>. The E3SM model can be accessed at  
635 <https://zenodo.org/records/12175988>. The dataset for machine learning trigger function can be accessed  
636 at <https://zenodo.org/records/12205917>. The dataset for machine learning wild fire can be accessed at  
637 <https://zenodo.org/records/12212258>.

Deleted: <https://doi.org/10.11578/E3SM/dc.20240301.3>  
(E3SM Project, 2024)

## 638 References

639 Bechtold, P., Chaboureaud, J.-P., Beljaars, A., Betts, A. K., Köhler, M., Miller, M., & Redelsperger, J.-L.  
640 (2004). The simulation of the diurnal cycle of convective precipitation over land in a global

643 model. *Quarterly Journal of the Royal Meteorological Society*, 130(604), 3119–3137.  
644 <https://doi.org/10.1256/qj.03.103>

645 Bogenschutz, P. A., Tang, S., Caldwell, P. M., Xie, S., Lin, W., & Chen, Y.-S. (2020). The E3SM version  
646 1 single-column model. *Geoscientific Model Development*, 13(9), 4443–4458.  
647 <https://doi.org/10.5194/gmd-13-4443-2020>

648 Brenowitz, N. D., & Bretherton, C. S. (2018). Prognostic validation of a neural network unified physics  
649 parameterization. *Geophysical Research Letters*, 45(12), 6289–6298.  
650 <https://doi.org/10.1029/2018gl078510>

651 Brenowitz, N. D., & Bretherton, C. S. (2019). Spatially extended tests of a neural network  
652 parametrization trained by coarse-graining. *Journal of Advances in Modeling Earth Systems*,  
653 11(8), 2728–2744. <https://doi.org/10.1029/2019ms001711>

654 Bush, M., Allen, T., Bain, C., Boutle, I., Edwards, J., Finnenkoetter, A., Franklin, C., Hanley, K., Lean,  
655 H., Lock, A., Manners, J., Mittermaier, M., Morcrette, C., North, R., Petch, J., Short, C., Vosper,  
656 S., Walters, D., Webster, S., ... Zerroukat, M. (2020). The first Met Office Unified Model–  
657 JULES Regional Atmosphere and Land configuration, RAL1. *Geoscientific Model Development*,  
658 13(4), 1999–2029. <https://doi.org/10.5194/gmd-13-1999-2020>

659 Chen, G., Wang, W., Yang, S., Wang, Y., Zhang, F., & Wu, K. (2023). A Neural Network-Based Scale-  
660 Adaptive Cloud-Fraction Scheme for GCMs. *Journal of Advances in Modeling Earth Systems*,  
661 15(6), e2022MS003415. <https://doi.org/10.1029/2022MS003415>

662 E3SM Project, D. (2024). *Energy Exascale Earth System Model v3.0.0* [Computer software]. [object  
663 Object]. <https://doi.org/10.11578/E3SM/DC.20240301.3>

664 Gerber, R., & Wasserman, H. (2013). *High Performance Computing and Storage Requirements for*  
665 *Biological and Environmental Research Target 2017* (LBNL-6256E). Lawrence Berkeley  
666 National Lab. (LBNL), Berkeley, CA (United States). <https://doi.org/10.2172/1171504>

667 Gettelman, A., Gagne, D. J., Chen, C.-C., Christensen, M. W., Lebo, Z. J., Morrison, H., & Gantos, G.  
668 (2021). Machine Learning the Warm Rain Process. *Journal of Advances in Modeling Earth*  
669 *Systems*, 13(2), e2020MS002268. <https://doi.org/10.1029/2020MS002268>

670 Gettelman, A., Truesdale, J. E., Bacmeister, J. T., Caldwell, P. M., Neale, R. B., Bogenschutz, P. A., &  
671 Simpson, I. R. (2019). The Single Column Atmosphere Model Version 6 (SCAM6): Not a Scam  
672 but a Tool for Model Evaluation and Development. *Journal of Advances in Modeling Earth*  
673 *Systems*, 11(5), 1381–1401. <https://doi.org/10.1029/2018MS001578>

674 Golaz, J.-C., Caldwell, P. M., Van Roekel, L. P., Petersen, M. R., Tang, Q., Wolfe, J. D., Abeshu, G.,  
675 Anantharaj, V., Asay-Davis, X. S., Bader, D. C., Baldwin, S. A., Bisht, G., Bogenschutz, P. A.,  
676 Branstetter, M., Brunke, M. A., Brus, S. R., Burrows, S. M., Cameron-Smith, P. J., Donahue, A.  
677 S., ... Zhu, Q. (2019). The DOE E3SM Coupled Model Version 1: Overview and Evaluation at  
678 Standard Resolution. *Journal of Advances in Modeling Earth Systems*, 11(7), 2089–2129.  
679 <https://doi.org/10.1029/2018MS001603>

680 Golaz, J.-C., Van Roekel, L. P., Zheng, X., Roberts, A. F., Wolfe, J. D., Lin, W., Bradley, A. M., Tang,  
681 Q., Maltrud, M. E., Forsyth, R. M., Zhang, C., Zhou, T., Zhang, K., Zender, C. S., Wu, M.,  
682 Wang, H., Turner, A. K., Singh, B., Richter, J. H., ... Bader, D. C. (2022). The DOE E3SM  
683 Model Version 2: Overview of the Physical Model and Initial Model Evaluation. *Journal of*  
684 *Advances in Modeling Earth Systems*, 14(12), e2022MS003156.  
685 <https://doi.org/10.1029/2022MS003156>

686 Han, Y., Zhang, G. J., Huang, X., & Wang, Y. (2020). A Moist Physics Parameterization Based on Deep  
687 Learning. *Journal of Advances in Modeling Earth Systems*, 12(9), e2020MS002076.  
688 <https://doi.org/10.1029/2020MS002076>

689 Hartmann, D. L., Blossey, P. N., & Dygert, B. D. (2019). Convection and Climate: What Have We  
690 Learned from Simple Models and Simplified Settings? *Current Climate Change Reports*, 5(3),  
691 196–206. <https://doi.org/10.1007/s40641-019-00136-9>

692 Hourdin, F., Mauritsen, T., Gettelman, A., Golaz, J.-C., Balaji, V., Duan, Q., Folini, D., Ji, D., Klocke,  
693 D., Qian, Y., Rauser, F., Rio, C., Tomassini, L., Watanabe, M., & Williamson, D. (2017). The Art  
694 and Science of Climate Model Tuning. *Bulletin of the American Meteorological Society*, *98*(3),  
695 589–602. <https://doi.org/10.1175/BAMS-D-15-00135.1>

696 Huang, H., Xue, Y., Li, F., & Liu, Y. (2020). Modeling long-term fire impact on ecosystem  
697 characteristics and surface energy using a process-based vegetation–fire model SSiB4/TRIFFID-  
698 Fire v1.0. *Geoscientific Model Development*, *13*(12), 6029–6050. [https://doi.org/10.5194/gmd-13-](https://doi.org/10.5194/gmd-13-6029-2020)  
699 [6029-2020](https://doi.org/10.5194/gmd-13-6029-2020)

700 Krasnopolsky, V. M., Fox-Rabinovitz, M. S., & Belochitski, A. A. (2013). Using ensemble of neural  
701 networks to learn stochastic convection parameterizations for climate and numerical weather  
702 prediction models from data simulated by a cloud resolving model. *Advances in Artificial Neural*  
703 *Systems*, *2013*, 5–5. <https://doi.org/10.1155/2013/485913>

704 Lee, M.-I., Schubert, S. D., Suarez, M. J., Held, I. M., Lau, N.-C., Ploshay, J. J., Kumar, A., Kim, H.-K.,  
705 & Schemm, J.-K. E. (2007). An Analysis of the Warm-Season Diurnal Cycle over the Continental  
706 United States and Northern Mexico in General Circulation Models. *Journal of*  
707 *Hydrometeorology*, *8*(3), 344–366. <https://doi.org/10.1175/JHM581.1>

708 O’Gorman, P. A., & Dwyer, J. G. (2018). Using machine learning to parameterize moist convection:  
709 Potential for modeling of climate, climate change, and extreme events. *Journal of Advances in*  
710 *Modeling Earth Systems*, *10*(10), 2548–2563. <https://doi.org/10.1029/2018ms001351>

711 Randall, D. A. (2013). Beyond deadlock. *Geophysical Research Letters*, *40*(22), 5970–5976.  
712 <https://doi.org/10.1002/2013GL057998>

713 Randall, D., Khairoutdinov, M., Arakawa, A., & Grabowski, W. (2003). Breaking the Cloud  
714 Parameterization Deadlock. *Bulletin of the American Meteorological Society*, *84*(11), 1547–1564.  
715 <https://doi.org/10.1175/BAMS-84-11-1547>

716 Rasp, S., Pritchard, M. S., & Gentine, P. (2018). Deep learning to represent subgrid processes in climate  
717 models. *Proceedings of the National Academy of Sciences*, *115*(39), 9684–9689.  
718 <https://doi.org/10.1073/pnas.1810286115>

719 Schär, C., Fuhrer, O., Arteaga, A., Ban, N., Charpiloz, C., Girolamo, S. D., Hentgen, L., Hoefler, T.,  
720 Lapillonne, X., Leutwyler, D., Osterried, K., Panosetti, D., Rüdüsühli, S., Schlemmer, L.,  
721 Schulthess, T. C., Sprenger, M., Ubbiali, S., & Wernli, H. (2020). Kilometer-Scale Climate  
722 Models: Prospects and Challenges. *Bulletin of the American Meteorological Society*, *101*(5),  
723 E567–E587. <https://doi.org/10.1175/BAMS-D-18-0167.1>

724 Swann, H. (2001). Evaluation of the mass-flux approach to parametrizing deep convection. *Quarterly*  
725 *Journal of the Royal Meteorological Society*, *127*(574), 1239–1260.  
726 <https://doi.org/10.1002/qj.49712757406>

727 Walters, D., Boutle, I., Brooks, M., Melvin, T., Stratton, R., Vosper, S., Wells, H., Williams, K., Wood,  
728 N., Allen, T., Bushell, A., Copsey, D., Earnshaw, P., Edwards, J., Gross, M., Hardiman, S.,  
729 Harris, C., Heming, J., Klingaman, N., ... Xavier, P. (2017). The Met Office Unified Model  
730 Global Atmosphere 6.0/6.1 and JULES Global Land 6.0/6.1 configurations. *Geoscientific Model*  
731 *Development*, *10*(4), 1487–1520. <https://doi.org/10.5194/gmd-10-1487-2017>

732 Wang, X., Han, Y., Xue, W., Yang, G., & Zhang, G. J. (2022). Stable climate simulations using a realistic  
733 general circulation model with neural network parameterizations for atmospheric moist physics  
734 and radiation processes. *Geoscientific Model Development*, *15*(9), 3923–3940.  
735 <https://doi.org/10.5194/gmd-15-3923-2022>

736 Webster, S., Uddstrom, M., Oliver, H., & Vosper, S. (2008). A high-resolution modelling case study of a  
737 severe weather event over New Zealand. *Atmospheric Science Letters*, *9*(3), 119–128.  
738 <https://doi.org/10.1002/asl.172>

739 Xu, K.-M., & Randall, D. A. (1996). A Semiempirical Cloudiness Parameterization for Use in Climate  
740 Models. *Journal of the Atmospheric Sciences*, *53*(21), 3084–3102. [https://doi.org/10.1175/1520-0469\(1996\)053<3084:ASCPFU>2.0.CO;2](https://doi.org/10.1175/1520-0469(1996)053<3084:ASCPFU>2.0.CO;2)

742 Zhang, T., Lin, W., Vogelmann, A. M., Zhang, M., Xie, S., Qin, Y., & Golaz, J.-C. (2021). Improving  
743 Convection Trigger Functions in Deep Convective Parameterization Schemes Using Machine  
744 Learning. *Journal of Advances in Modeling Earth Systems*, 13(5), e2020MS002365.  
745 <https://doi.org/10.1029/2020MS002365>

746 Zhang, T., Morcrette, C., Zhang, M., Lin, W., Xie, S., Liu, Y., Weverberg, K. V., & Rodrigues, J. (2024).  
747 *tzhang-ccs/ML4ESM: ML4ESM\_v1* (Version v1) [Computer software]. [object Object].  
748 <https://doi.org/10.5281/ZENODO.11005103>  
749